

Exotic Stable Branches with Efficient TOV Sequences

Reed Essick^{1,2,3,*}

¹Canadian Institute for Theoretical Astrophysics, 60 St. George St, Toronto, Ontario M5S 3H8

²Department of Physics, University of Toronto, 60 St. George Street, Toronto, ON M5S 1A7

³David A. Dunlap Department of Astronomy, University of Toronto, 50 St. George Street, Toronto, ON M5S 3H4

Modern inference schemes for the neutron star equation of state (EoS) require large numbers of stellar models constructed with different EoS, and these stellar models must capture all the behavior of stable stars. I introduce termination conditions for sequences of stellar models for cold, non-rotating neutron stars that are guaranteed to identify all stable stellar configurations up to arbitrarily large central pressures along with an efficient algorithm to build accurate interpolators for macroscopic properties. I explore the behavior of stars with both high- and low-central pressures. Interestingly, I find that EoS with monotonically increasing sound-speed can produce multiple stable branches (twin stars) and that large phase transitions at high densities can produce stable branches at nearly any mass scale, including sub-solar masses, while still supporting stars with $M > 2 M_\odot$. I conclude with some speculation about the astrophysical implications of this behavior.

INTRODUCTION

Neutron stars (NSs) are extremely dense stellar remnants typically observed with masses between $1\text{--}2 M_\odot$ with radii ~ 12 km [1]. As such, NSs reach characteristic densities¹ $\langle \rho \rangle = 3M/4\pi R^3 \approx 5 \cdot 10^{14}$ g/cm³, roughly twice the density of atomic nuclei (nuclear saturation density: $n_{\text{sat}} \approx 0.16$ fm⁻³ or $\rho_{\text{sat}} = m_n n_{\text{sat}} \approx 2.8 \times 10^{14}$ g/cm³ where m_n is the nucleon rest-mass). Therefore, many-body nuclear interactions play a key role in NS structure. At the same time, NSs can reach compactness $C = M/R \sim 1/4$, which is close to the upper limit expected from a Schwarzschild Black Hole (BH): $C_{\text{Sch}} = 1/2$. Clearly, then, relativistic effects should also be significant.

The structure of cold, non-rotating NSs is governed by the Tolman-Oppenheimer-Volkoff (TOV) equations [2, 3]²

$$\frac{dm}{dr} = 4\pi r^2 \varepsilon \quad (1)$$

$$\frac{dp}{dr} = -\frac{m\varepsilon}{r^2} \left(1 + \frac{p}{\varepsilon}\right) \left(1 + \frac{4\pi r^3 p}{m}\right) \left(1 - \frac{2m}{r}\right)^{-1} \quad (2)$$

where p is the pressure, ε the energy density, r the radial coordinate, and m the enclosed gravitational mass (distinct from the enclosed rest-mass as it includes the gravitational binding energy). Because NSs are believed to be supported primarily by degeneracy pressure, these equations are closed with a barytropic equation of state

(EoS) that specifies p as a function of ε .³ Finally, the TOV equations are solved with boundary values in the center and at the surface of the star:

$$\lim_{r \rightarrow 0^+} \frac{dp}{dr} = 0 \quad (\text{center}) \quad (3)$$

$$\lim_{r \rightarrow R^-} p = 0 \quad (\text{surface}) \quad (4)$$

The only remaining free parameter is the central pressure (p_c), and one can construct relationships between, e.g., the radius (R) and gravitational mass ($M = m(R)$) by repeatedly solving for a sequence of p_c . One is often instructed to continue this process until a local maximum in M is observed, which corresponds to a loss of stability [6–9]. Because only stable stellar configurations can persist in nature, the sequence of stellar models is terminated at that point.

The fact that cold, non-rotating NSs are bounded below a maximum mass (M_{TOV}) is often referred to as the TOV limit, and the stable stellar models that exist with $dM/dp_c > 0$ and p_c less than the central pressure at the TOV limit (p_{TOV}) are called a *stable branch* of the, e.g., M - R curve.

However, in general, the EoS can support multiple stable branches. Famously, EoS with strong 1st-order phase transitions can yield stellar sequences which lose stability when p_c reaches the onset of the phase transition and regain stability when p_c is slightly above the end of the phase transition [13]. This can lead to multiple stars with the same M but different R (*twin stars*). Fig. 1 shows a few examples. See, e.g., Refs. [13–16] for more discussion.

Importantly, the naive termination condition for the TOV sequence fails to capture the physics of phase transitions (i.e., the presence of twin stars). It is clear, then,

¹ I write expressions in units where $G = c = 1$ but provide explicit units when relevant.

² It is common practice to solve the TOV equations in a slightly different form, sometimes called the (log)enthalpy formulation [4]. See also Ref. [5] for a recent review of numerical techniques. I find that the enthalpy formulation provides a factor of $\sim 5\text{--}10$ speedup compared to the “standard” formulation described above.

³ The EoS can also be specified in terms of other thermodynamic variables, like the number density (n), the chemical potential ($\mu = d\varepsilon/dn = (\varepsilon + p)/n$), or the sound-speed ($c_s^2 = dp/d\varepsilon$).

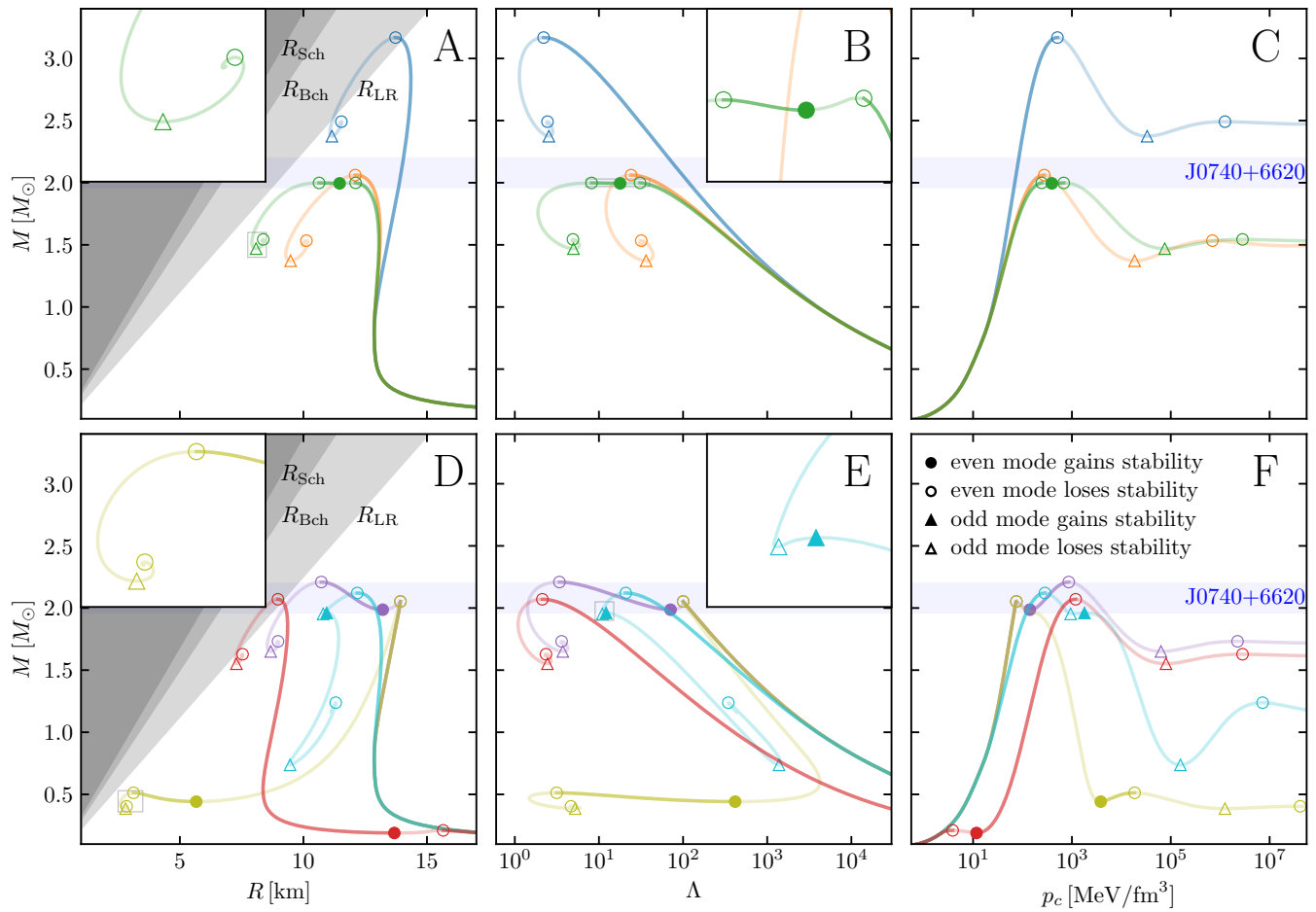


FIG. 1. EoS based on chiral effective field theory (χ EFT [10]) below $p = 2.2 \text{ MeV}/\text{fm}^3$ (*top*) without and (*bottom*) with 1st-order phase transitions. I show (*left*) M - R , (*middle*) M - Λ (tidal deformability), and (*right*) M - p_c curves. Stable branches are dark solid lines and unstable branches are light lines of the same color. The points where stability changes are: (*circles*) even modes ($n = 0, 2, \dots$) and (*triangles*) odd modes ($n = 1, 3, \dots$) with (*filled symbols*) where stability is regained and (*empty symbols*) where stability is lost. For clarity, I only show modes with $n \leq 2$. I also show the Schwarzschild ($R_{\text{Sch}} = 2M$), Buchdahl ($R_{\text{Bch}} = 9M/4$), and light ring ($R_{\text{LR}} = 3M$) radii along with the approximate 90% credible region for the mass of J0740+6620 [11, 12].

that one must continue to solve the TOV equations for p_c above the first point where $dM/dp_c = 0$. This begs the question of when, if ever, one can be confident that they have reached the end of the final stable branch. This letter provides a new termination condition based on the stability of high-density stars, which automatically detects the beginning and the end of all stable NS branches.

Additionally, I provide an efficient algorithm to construct stellar sequences. Modern inference schemes for the EoS can require 10^4 - 10^6 EoS proposals. Even modest reductions in the number of stellar models required per EoS can result in significant overall savings, and my algorithm achieves an order of magnitude reduction in computational cost per EoS compared to other algorithms with, e.g., uniform grid placements in $\ln p_c$. Accurate interpolators for macroscopic relations can be achieved in $O(500)$ ms/EoS on a modern laptop, making it possible

to analyze large EoS sets with minimal computational resources in only a few hours.

TOV TERMINATION CONDITIONS

As shown in Fig. 1, the high-density TOV sequence always approaches a fixed point

$$M_{\odot} \equiv \lim_{p_c \rightarrow \infty} M \quad (5)$$

through a counterclockwise spiral in the M - R plane.⁴ The location of the spiral depends on the EoS, but it always contains many local extrema in M . The relevant

⁴ Similar behavior can also appear in Newtonian gravity [17, 18].

“static” stability criteria [6–9] can be summarized as follows: a M - R curve that bends counterclockwise corresponds to a mode losing stability, while one that bends clockwise corresponds to a mode regaining stability. As discussed extensively in Harrison *et al.* [7], the fact that $dM/dp_c > 0$ for some parts of the spiral does not guarantee stability, and instead each subsequent extremum of M within the spiral corresponds to another stellar eigenmode becoming unstable in order of increasing number of radial nodes (n). Harrison *et al.* [7] even derives analytic expressions for the M - p_c curve when c_s^2 is a constant at large p : M is a damped-sinusoid in $\ln p_c$, and there is an infinite sequence of branches where $dM/dp_c > 0$ above p_{TOV} .

At very large p_c , I find that once the first harmonic ($n = 1$) becomes unstable, the star can never become completely stable again. The $n = 1$ mode may momentarily restabilize (panel E of Fig. 1), but the fundamental mode ($n = 0$) will not restabilize even if the EoS is causal ($c_s^2 = 1$).

In the presence of twin stars, we may see several extrema in M corresponding to $n = 0$ losing and regaining stability. Nevertheless, after $n = 0$ becomes unstable “for good,” the next mode to become unstable is $n = 1$. This corresponds to a local minimum in M with $dR/dp_c > 0$. At this point, additional extrema never correspond to $n = 0$ regaining stability. Said another way, while $n = 0$ can regain stability at high p_c when $n = 1$ is still stable, it cannot once $n = 1$ is unstable. If one detects an unstable $n = 1$, then, this signals the final spiral towards M_\odot and that all stars with larger p_c are unstable.

Fig. 1 shows the behavior of M - R , M - Λ (tidal deformability), and M - p_c for several EoS with different high-density behavior. Annotations label which modes change stability at each local extremum in M . I discuss some of the qualitative differences in these M - R curves and their relationship to the high-density EoS below.

At low p_c , one also expects a minimum NS mass associated with $n = 0$ regaining stability after the white dwarf (WD) branch loses stability [7]. This manifests as a local minimum in M with $dR/dp_c < 0$. Typically, this occurs for p_c low enough to be in the NS crust (i.e., the whole star is “crust”), where the physics is relatively well understood and one does not have to worry about exotic behavior.

ADAPTIVE TOV SEQUENCES

Given stopping criteria for the TOV sequence at both high and low p_c , one must determine how to efficiently construct an array of p_c that yields useful M - R and M - Λ curves. The following adaptive algorithm accomplishes this by placing additional stellar models only where errors in the interpolated curves are large.

The algorithm operates via recursive bisection. Given

an initial min- and max- p_c , along with corresponding stellar models, it generates a new p_c (mid- p_c , the geometric mean of min- and max- p_c), solves for the associated stellar model, and checks the accuracy of a linear interpolator (based on the min- and max- p_c) at mid- p_c .⁵ If the interpolator passes a relative error tolerance, the algorithm terminates and returns the stellar models at min-, mid-, and max- p_c . Otherwise, it returns the union of recursive call on the two segments defined from min- to mid- p_c and from mid- to max- p_c . In this way, additional models are only generated where the corresponding interpolator has relatively poor performance. Compared to a grid with models placed uniformly in $\ln p_c$, I see as much as a factor of ~ 10 reduction in the number of models needed to achieve the same relative interpolator error at all points along M - R curves.

This algorithm converges best when the function is reasonably smooth between min- and max- p_c , although it reliably detects kinks and bends as well. As such, it can be seeded with an initial coarse grid in p_c and iteratively applied to each segment.⁶

After the recursive routine terminates, the algorithm checks whether the termination conditions at high p_c ($n = 1$ mode loses stability) and low p_c ($n = 0$ mode regains stability) are observed within the existing set of stellar models. If not, it extends the range of p_c geometrically as needed and calls the recursive routine on the new segments. This is repeated until the termination conditions are observed (or the algorithm reaches values of p_c larger than any p recorded within the tabulated EoS).

Importantly, when extending the set of stellar models to lower p_c , the algorithm only looks for the termination condition within the new set of low- p_c models. Otherwise, it may prematurely exit if there are multiple stable branches at higher p_c . Fig. 1 shows such a EoS with a phase transition at low densities (just above n_{sat}) that yields a short unstable branch at $M \sim 0.25 M_\odot$. Again, to reliably identify the presence of such features, one must instantiate the search for the end of low- p_c stable branches at $n_c \lesssim n_{\text{sat}}$, often well within the crust.

This issue does not arise when extending the sequence to higher p_c as long as one focuses on the range of p_c relevant for NSs and stays well above what is relevant for WDs ($p_c \sim 6 \times 10^{-7} \text{ MeV/fm}^3$).

In principle, this algorithm could be instantiated with a single p_c and rely on the extension prescriptions to both higher and lower p_c . However, the geometric expansion *de facto* results in less-well-optimized grid placement than allowing the adaptive algorithm to choose where to

⁵ More complicated interpolators could be used, but the speed and simplicity of linear interpolation work well in practice.

⁶ The initial grid could contain only two points, though, in which case the adaptive grid would be constructed throughout the entire domain of stellar models.

add more grid points throughout a wider initial range. I find that beginning with a reasonable initial guess for the min- and max- p_c requires $O(10\%)$ fewer stellar models compared to relying only on the geometric expansion.

Altogether, my implementation [19] requires $O(3)$ ms/model on a modern laptop (11th Gen Intel i7-1185G7 clocked at 3 GHz). Reliable interpolators for M - R can be constructed with with ~ 100 -150 models (interpolators for M - Λ require more points; see discussion below), yielding an runtime of $\lesssim O(500)$ ms/EoS.⁷

However, a significant fraction of the stellar models produced have low p_c (large R and Λ). If one is only interested in, e.g., stars with $M \gtrsim 0.5 M_\odot$, then many of the models at lower p_c can be skipped. The reduced range may need $\lesssim 50$ models for accurate interpolation, but this requires user expertise to guarantee that min- p_c is chosen appropriately.

Finally, solving for only (M, R) takes $O(3)$ ms/model whereas solving for (M, R, Λ) takes $O(6)$ ms/model. Additionally, the adaptive grid often requires fewer p_c to converge for just M - R compared to M - Λ . The difference can be as large as a factor of ~ 5 , but more commonly is a factor of $\lesssim 2$. As such, it is not uncommon to find a combined factor of several speedup when only solving for (M, R) . One might achieve a net speedup by first solving for (M, R) with a coarse interpolator to identify the relevant range of p_c and then re-solving with a finer resolution for (M, R, Λ) only within the relevant range. This may be particularly helpful if some EoS will be discarded based on information available from the M - R curve, like M_{TOV} . In this case, one would never have to solve for M - Λ for some EoS. However, I leave a precise quantification of the potential speedup to future work.

Equipped with this algorithm for rapid and reliable TOV sequences, I now explore exotic behavior at both low- and high- p_c .

EXOTIC LOW-DENSITY BEHAVIOR

As briefly discussed before, the EoS can support multiple stable branches at low p_c while still matching *ab initio* theory [10] at $n \lesssim n_{\text{sat}}$. In particular, there can be a phase transition just above n_{sat} that is consistent with astrophysical observations, which currently allow phase transitions (and multiple stable branches) at $M \lesssim M_\odot$ and/or $M \gtrsim 2 M_\odot$ [1, 13]. In fact, although far from being certain, if a large slope parameter at n_{sat} ($L \gtrsim 100$ MeV) is observed experimentally, such a phase transition just above n_{sat} could actually be preferred by current observations [20, 21].

Fig. 1 shows an example of such an EoS. Often, small $R(1.4 M_\odot)$ are associated with this behavior; only the EoS with a low- p phase transition supports $R(1.4 M_\odot) < 10$ km in this (admittedly small) sample.

EXOTIC HIGH-DENSITY BEHAVIOR

Fig. 1 also shows various high-density behavior, including stiff ($c_s^2 \sim 1$) and soft ($c_s^2 \sim 1/3$) EoS both with and without 1st-order phase transitions. All stellar sequences eventually end in a counterclockwise spiral. However, the path by which the high-density models enter this spiral can vary. I focus on EoS that approximately satisfy current observations constraints (i.e., follow χ EFT at low densities and have $R(1.4 M_\odot) \sim 12.5$ km, $M_{\text{TOV}} \gtrsim 2 M_\odot$).

The vanilla behavior is as follows: $n = 0$ becomes unstable, then M decreases and enters a spiral. The spiral is always centered on $M_\odot < M_{\text{TOV}}$, and the M - R curves never cross themselves (i.e., *identical* twin stars are not physical). It is interesting that EoS with $c_s^2 \sim 1$ for $p \sim p_{\text{TOV}}$ produce R_{TOV} comparable to (and smaller than!) their light-ring ($R_{\text{LR}} = 3M$). This could create a (small) resonating cavity like those invoked to motivate searches for gravitational-wave echoes [22, 23].

The presence of twin stars only moderately complicates this behavior: $n = 0$ can regain stability, and the second stable branch can, but does not have to, reach higher M than the first stable branch. Again, later stable branches with $c_s^2 \sim 1$ can terminate near R_{LR} .

If a phase transition occurs at $p > p_{\text{TOV}}$, it can still cause a change in stability. However, $n = 1$ loses and regains stability rather than $n = 0$. In this case, the star as a whole remains unstable (panel E in Fig. 1).

Counter to claims made in the literature, it is also possible to generate twin stars *without* a 1st-order phase transition (Fig. 2). Even EoS with monotonically increasing c_s^2 can produce twin stars.⁸ This phenomenology is difficult (but not impossible!) to achieve while satisfying current observational constraints (panel B in Fig. 1). Relaxing the requirement that $M_{\text{TOV}} \gtrsim 2 M_\odot$ allows a much wider range of EoS with monotonic c_s^2 to produce twin stars (Fig. 2).

Finally, phase transitions at high p with large latent energies can generate stable branches with $M \ll M_{\text{TOV}}$ and $R \ll R_{\text{TOV}}$ if $c_s^2 \sim 1$ beyond the transition (Figs. 1 and 3). These stars can have central pressures much higher than p_{TOV} , often \gtrsim GeV/fm³. I will refer to them as high- p_c objects, or HiPOs. Without sufficient exploration of high- p_c TOV solutions, these branches

⁷ It takes longer to read the EoS table from and write the TOV solutions to disk.

⁸ For these EoS, c_s^2 behaves as one might expect for a 2nd-order phase transition.

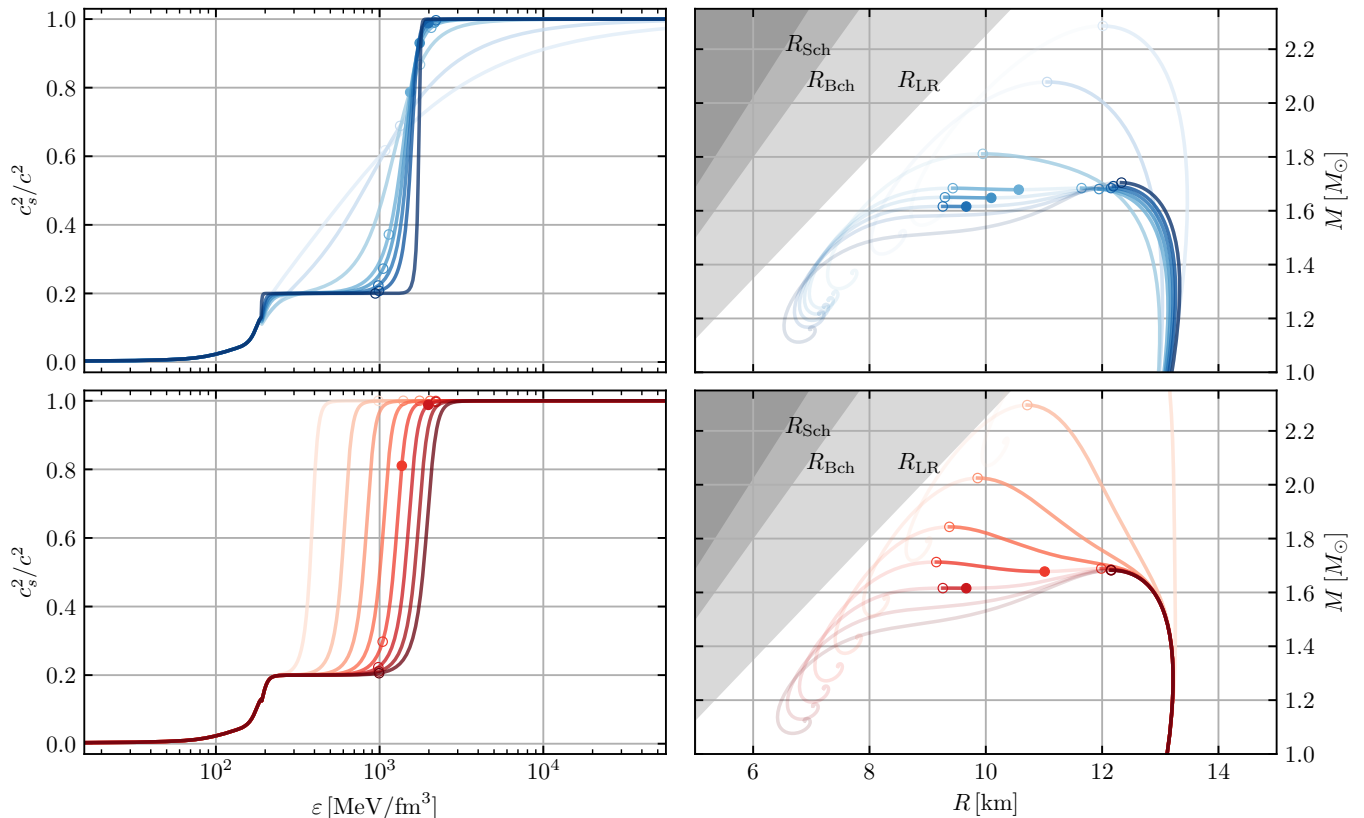


FIG. 2. EoS with monotonically increasing c_s^2 that produce twin stars: (*left*) c_s^2 vs. ε and (*right*) M vs. R . Stable and unstable branches are denoted as in Fig. 1. The ability of such EoS to support twin stars is a combination of (*top*) the smoothness of c_s^2 and (*bottom*) the size of the density range where c_s^2 is nearly constant. This behavior is reminiscent of 2nd-order phase transitions as there is a (near) discontinuity in $dc_s^2/d\varepsilon = d^2p/d\varepsilon^2$ rather than $c_s^2 = dp/d\varepsilon$. Although not shown here, EoS that support twin stars do so even if $c_s^2 \rightarrow 1/3$ at higher densities. I use examples with $M_{\text{TOV}} < 2 M_\odot$ to more clearly show the variety of behavior. Fig. 1 shows an example with $M_{\text{TOV}} \sim 2 M_\odot$.

could have easily been missed (i.e., there is a long unstable branch before the sequence regains stability). HiPO branches appear to be common if $c_s^2 \sim 1$ is allowed at large p . It may be possible to extend most EoS that satisfy astrophysical constraints with this type of high-density behavior, and recent proposals for how to incorporate theoretical predictions from perturbative quantum chromodynamics (pQCD [24]) invoke EoS like these. One can also tune the high- p EoS to place M_\odot at nearly any value $\lesssim M_{\text{TOV}}$. Reducing either the latent energy or density at which $c_s^2 \rightarrow 1/3$ tends to increase M_\odot and decrease the extent of the stable branch. Fig. 3 shows the typical behavior.

SUMMARY

Based on the stability of dense stars, I introduce improved termination conditions for sequences of stellar models. Together with an efficient algorithm to construct reliable interpolators, I explored the types of behaviors

observed at low- and high- p_c . Surprisingly, I find that

- an EoS can support twin stars even though c_s^2 always increases monotonically, and
- large phase transitions at high p can produce stable (HiPO) branches at much smaller (M, R) than the TOV limit with p_c near what is directly accessible with pQCD.

Both behaviors are possible while maintaining $M_{\text{TOV}} \gtrsim 2 M_\odot$ and reasonable radii. Their existence shows that more care may be needed in the literature⁹ when making claims that, e.g., the presence of twin stars robustly implies the presence of a 1st-order phase transition or that the presence of a sub-solar mass object with small Λ (observationally indistinguishable from a BH with $\Lambda_{\text{BH}} = 0$) is clear evidence for sub-solar mass BHs [27, 28]. Instead, twin stars near M_{TOV} do not require a 1st-order

⁹ Or, at least, within my body of work [13, 20, 21, 25, 26].

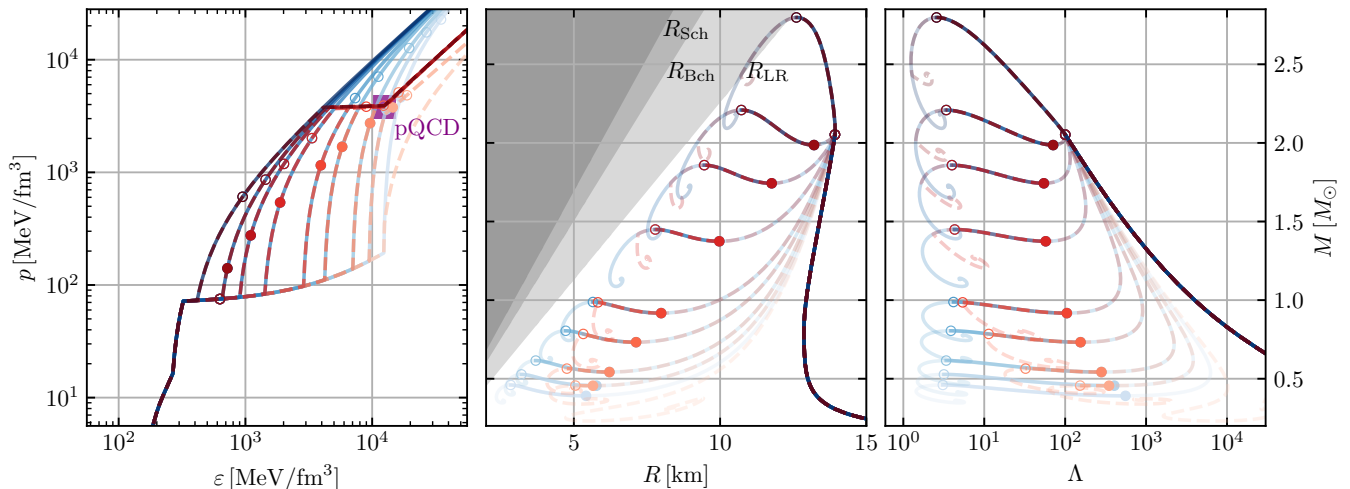


FIG. 3. EoS with high-density phase transitions and HiPO branches: (*left*) p vs. ε , (*center*) M vs. R , and (*right*) Λ vs. M . Stability is indicated as in Figs. 1 and 2. I show (*solid lines*) EoS with $c_s^2 = 1$ up to arbitrarily high densities and (*dashed lines*) EoS that match (*purple square*) approximates pQCD predictions at $\varepsilon \approx 12.5 \text{ GeV/fm}^3$ for p and c_s^2 [24]. The single EoS that fails to support a HiPO branch does so because $c_s^2 = 1/3$ at all densities above its phase transition (i.e., c_s^2 never reaches ~ 1). This is also the only EoS which fails to match the pQCD prediction.

phase transition, and there can be stable NS branches with $\Lambda \sim O(10)$ and $M \lesssim M_\odot$.¹⁰

That being said, even if HiPO branches exist, the range of masses a single EoS can support is limited. While it may be possible to produce an EoS that matches the mass of any individual object with $\Lambda \sim 0$, it may be difficult to explain the observation of a population of compact objects over a range of M . Alternative explanations would not be ruled out, though, including complex dark sectors that support “mirror stars” [29].

Taking the HiPO branches at face value, let us consider how one might form such a star dynamically. The jump from the “normal” NS branch ($p < p_{\text{TOV}}$) to the HiPO branch is in many ways analogous to the jump from the WD branch to the NS branches. There is a reduction in the number of particles (N) within the star¹¹

$$N = \int_0^R dr \frac{4\pi r^2 n}{\sqrt{1 - 2m/r}} \quad (6)$$

implying that a star collapsing from M_{TOV} to the HiPO branch would have to shed a significant amount of mass, as much as $O(1)M_\odot$. This could happen in a process analogous to a core-collapse supernova (CCSN),¹² al-

though it is unclear whether the HiPO branch could actually launch a shock in the same way that a proto-NS is thought to within CCSN. The infalling matter could overwhelm the HiPO branch and cause direct collapse to a BH. Also, Fig. 3 shows that some HiPO branches have $R \sim 2M_{\text{TOV}}$, meaning that the star would have to shed a significant amount of energy within the dynamical timescale of the collapse to avoid forming a trapped surface. Detailed simulations will likely be needed.

Interestingly, if one assumes the rest-mass per particle is the same on both the normal and HiPO branches, essentially all of the HiPO branches are less bound per particle than the normal branch ($(Nm_n - M)/N$ is smaller). However, if the particles produced in the phase transition instead have a rest-mass comparable to the chemical potential at the onset of the transition ($\mu_{\text{onset}} \sim 1.3m_n$ in Fig. 3, not dissimilar to some excited baryonic states [32]) and that most of the particles in HiPOs are of the exotic type, then the HiPO branch can be much more tightly bound per particle than any normal NS. This is, again, analogous to the way that WDs collapse to NSs: the electron is lighter than a nucleon, and NSs are more tightly bound than WDs.

Finally, taking the collapse scenario seriously, I estimate the total amount of energy that would be released as the difference between the initial and final states. Some (very) rough bounds can be set by assuming that the rest-mass from the difference in particle numbers between the TOV star and the HiPO branch is radiated as nucleons or that no rest-mass is radiated:

$$M_{\text{TOV}} - (M + (N_{\text{TOV}} - N)m_n) \leq \Delta E \leq M_{\text{TOV}} - M \quad (7)$$

Depending on the high- p EoS, this yields $\Delta E \sim 0.2-$

¹⁰ As such, more care is also warranted with statements that $p > p_{\text{TOV}}$ is both “unobserved and unobservable” [13], as the presence and/or absence of such branches directly constrains the high- p EoS.

¹¹ See the discussion of “pumping up the central density” in Harrison *et al.* [7].

¹² See also quark nova [30, 31], which similarly posit a transition from a NS to a more compact strange star.

$0.6 M_{\odot} \sim 10^{53}\text{-}10^{54}$ ergs, which is larger than typical CCSN, but only by a few orders of magnitude.

It may be plausible, then, that a subpopulation of electromagnetic transients could in fact be the collapse from normal NSs to HiPOs. The ejected mass would be considerably lower than for CCSN, though, as there is much less initial stellar material. However, it may have a very large kinetic energy. Additionally, the ejected mass would likely be very neutron rich, which may yield light-curves closer to a kilonova than a CCSN (faster decay rate, dimmer, and redder as radiation may be trapped by the high-opacity from r -process elements). The rate of such events could be quite low, though, as not all NSs are likely to undergo this process. An upper bound can be set by the rate of regular CCSN, but this is likely not particularly constraining.

I am deeply indebted to Chris Matzner, Bob Wald and Daniel Holz for discussions and suggested reading during the preparation of this manuscript. I also thank David Curtin and Janosz Dewberry for helpful discussions.

R.E. is supported by the Natural Sciences & Engineering Research Council of Canada (NSERC) through a Discovery Grant (RGPIN-2023-03346).

Implementations of these algorithms are available in **universality** [19]. This study would not have been possible without the following software: **numpy** [33], **scipy** [34], and **matplotlib** [35].

* E-mail: essick@cita.utoronto.ca

- [1] I. Legred, K. Chatziioannou, R. Essick, S. Han, and P. Landry, Impact of the PSR J0740+6620 radius constraint on the properties of high-density matter, *Phys. Rev. D* **104**, 063003 (2021), [arXiv:2106.05313](https://arxiv.org/abs/2106.05313) [[astro-ph.HE](#)].
- [2] J. R. Oppenheimer and G. M. Volkoff, On massive neutron cores, *Phys. Rev.* **55**, 374 (1939).
- [3] R. C. Tolman, Static solutions of einstein's field equations for spheres of fluid, *Phys. Rev.* **55**, 364 (1939).
- [4] L. Lindblom, The relativistic inverse stellar structure problem, *AIP Conference Proceedings* **1577**, 153 (2014), https://pubs.aip.org/aip/acp/article-pdf/1577/1/153/11408814/153.1_online.pdf.
- [5] W. Kastaun and F. Ohme, Modern tools for computing neutron star properties, (2024), [arXiv:2404.11346](https://arxiv.org/abs/2404.11346) [[gr-qc](#)].
- [6] J. M. Bardeen, K. S. Thorne, and D. W. Meltzer, A Catalogue of Methods for Studying the Normal Modes of Radial Pulsation of General-Relativistic Stellar Models, *Astrophys. J.* **145**, 505 (1966).
- [7] B. K. Harrison, K. S. Thorne, M. Wakano, and J. A. Wheeler, *Gravitation Theory and Gravitational Collapse* (1965).
- [8] R. Sorkin, A Criterion for the Onset of Instability at a Turning Point, *Astrophys. J.* **249**, 254 (1981).
- [9] R. D. Sorkin, A Stability Criterion for Many Parameter Equilibrium Families, *Astrophys. J.* **257**, 847 (1982).
- [10] J. Keller, K. Hebeler, and A. Schwenk, Nuclear equation of state for arbitrary proton fraction and temperature based on chiral effective field theory and a gaussian process emulator, *Phys. Rev. Lett.* **130**, 072701 (2023).
- [11] H. T. Cromartie *et al.*, Relativistic Shapiro delay measurements of an extremely massive millisecond pulsar, *Nature Astron.* **4**, 72 (2019), [arXiv:1904.06759](https://arxiv.org/abs/1904.06759).
- [12] E. Fonseca *et al.*, Refined Mass and Geometric Measurements of the High-mass PSR J0740+6620, *Astrophys. J. Lett.* **915**, L12 (2021), [arXiv:2104.00880](https://arxiv.org/abs/2104.00880) [[astro-ph.HE](#)].
- [13] R. Essick, I. Legred, K. Chatziioannou, S. Han, and P. Landry, Phase transition phenomenology with non-parametric representations of the neutron star equation of state, *Phys. Rev. D* **108**, 043013 (2023).
- [14] M. Alford, M. Braby, M. Paris, and S. Reddy, Hybrid stars that masquerade as neutron stars, *Astrophys. J.* **629**, 969 (2005), [arXiv:nucl-th/0411016](https://arxiv.org/abs/nucl-th/0411016).
- [15] M. G. Alford, S. Han, and M. Prakash, Generic conditions for stable hybrid stars, *Phys. Rev. D* **88**, 083013 (2013).
- [16] D. Mroczek, M. C. Miller, J. Noronha-Hostler, and N. Yunes, Nontrivial features in the speed of sound inside neutron stars, (2023), [arXiv:2309.02345](https://arxiv.org/abs/2309.02345) [[astro-ph.HE](#)].
- [17] W. B. Bonnar, Boyle's Law and Gravitational Instability, *Monthly Notices of the Royal Astronomical Society* **116**, 351 (1956), <https://academic.oup.com/mnras/article-pdf/116/3/351/8074473/mnras116-0351.pdf>.
- [18] R. Ebert, Über die Verdichtung von H I-Gebieten. Mit 5 Textabbildungen, *Zeitschrift für Astrophysik* **37**, 217 (1955).
- [19] R. Essick, **universality**, <https://github.com/reedessick/universality> (2024).
- [20] R. Essick, I. Tews, P. Landry, and A. Schwenk, Astrophysical Constraints on the Symmetry Energy and the Neutron Skin of Pb208 with Minimal Modeling Assumptions, *Phys. Rev. Lett.* **127**, 192701 (2021), [arXiv:2102.10074](https://arxiv.org/abs/2102.10074) [[nucl-th](#)].
- [21] R. Essick, P. Landry, A. Schwenk, and I. Tews, Detailed examination of astrophysical constraints on the symmetry energy and the neutron skin of Pb208 with minimal modeling assumptions, *Phys. Rev. C* **104**, 065804 (2021), [arXiv:2107.05528](https://arxiv.org/abs/2107.05528) [[nucl-th](#)].
- [22] L. F. Longo Micchi, N. Afshordi, and C. Chirenti, How loud are echoes from exotic compact objects?, *Phys. Rev. D* **103**, 044028 (2021).
- [23] N. Oshita and N. Afshordi, Probing microstructure of black hole spacetimes with gravitational wave echoes, *Phys. Rev. D* **99**, 044002 (2019).
- [24] O. Komoltsev, R. Somasundaram, T. Gorda, A. Kurkela, J. Margueron, and I. Tews, Equation of state at neutron-star densities and beyond from perturbative QCD, (2023), [arXiv:2312.14127](https://arxiv.org/abs/2312.14127) [[nucl-th](#)].
- [25] R. Essick, P. Landry, and D. E. Holz, Nonparametric Inference of Neutron Star Composition, Equation of State, and Maximum Mass with GW170817, *Phys. Rev. D* **101**, 063007 (2020), [arXiv:1910.09740](https://arxiv.org/abs/1910.09740) [[astro-ph.HE](#)].
- [26] R. Essick, I. Tews, P. Landry, S. Reddy, and D. E. Holz, Direct astrophysical tests of chiral effective field theory at supranuclear densities, *Phys. Rev. C* **102**, 055803 (2020).
- [27] F. Crescimbeni, G. Franciolini, P. Pani, and A. Riotto, Primordial black holes or else? Tidal tests on subsolar mass gravitational-wave observations, (2024), [arXiv:2402.18656](https://arxiv.org/abs/2402.18656) [[astro-ph.HE](#)].
- [28] J. Golomb, I. Legred, K. Chatziioannou, A. Abac, and

- T. Dietrich, Using Equation of State Constraints to Classify Low-Mass Compact Binary Mergers, (2024), [arXiv:2403.07697](https://arxiv.org/abs/2403.07697) [astro-ph.HE].
- [29] M. Hippert, J. Setford, H. Tan, D. Curtin, J. Noronha-Hostler, and N. Yunes, Mirror neutron stars, *Phys. Rev. D* **106**, 035025 (2022).
- [30] R. Ouyed, J. Dey, and M. Dey, Quark-Nova, *Astronomy and Astrophysics* **390**, L39 (2002), [arXiv:astro-ph/0105109](https://arxiv.org/abs/astro-ph/0105109) [astro-ph].
- [31] P. Jaikumar, B. S. Meyer, K. Otsuki, and R. Ouyed, Nucleosynthesis in neutron-rich ejecta from quark-novae, *Astronomy and Astrophysics* **471**, 227 (2007), [arXiv:nucl-th/0610013](https://arxiv.org/abs/nucl-th/0610013) [nucl-th].
- [32] R. L. Workman and Others (Particle Data Group), Review of Particle Physics, *PTEP* **2022**, 083C01 (2022).
- [33] C. R. Harris, K. J. Millman, S. J. van der Walt, R. Gommers, P. Virtanen, D. Cournapeau, E. Wieser, J. Taylor, S. Berg, N. J. Smith, R. Kern, M. Picus, S. Hoyer, M. H. van Kerkwijk, M. Brett, A. Haldane, J. F. del Río, M. Wiebe, P. Peterson, P. Gérard-Marchant, K. Sheppard, T. Reddy, W. Weckesser, H. Abbasi, C. Gohlke, and T. E. Oliphant, Array programming with NumPy, *Nature* **585**, 357 (2020).
- [34] P. Virtanen, R. Gommers, T. E. Oliphant, M. Haberland, T. Reddy, D. Cournapeau, E. Burovski, P. Peterson, W. Weckesser, J. Bright, S. J. van der Walt, M. Brett, J. Wilson, K. J. Millman, N. Mayorov, A. R. J. Nelson, E. Jones, R. Kern, E. Larson, C. J. Carey, Í. Polat, Y. Feng, E. W. Moore, J. VanderPlas, D. Laxalde, J. Perktold, R. Cimrman, I. Henriksen, E. A. Quintero, C. R. Harris, A. M. Archibald, A. H. Ribeiro, F. Pedregosa, P. van Mulbregt, and SciPy 1.0 Contributors, SciPy 1.0: Fundamental Algorithms for Scientific Computing in Python, *Nature Methods* **17**, 261 (2020).
- [35] J. D. Hunter, Matplotlib: A 2d graphics environment, *Computing in Science & Engineering* **9**, 90 (2007).